On metastable regimes of dynamic wetting

2002 J. Phys.: Condens. Matter 14 319

(http://iopscience.iop.org/0953-8984/14/3/303)

INSTITUTE OF PHYSICS PUBLISHING JOURNAL OF PHYSICS: CONDENSED MATTER

J. Phys.: Condens. Matter **14** (2002) 319–330 PII: S0953-8984(02)24546-4

On metastable regimes of dynamic wetting

Yulii D Shikhmurzaev

Department of Applied Mathematics, University of Birmingham, Birmingham B15 2TT, UK

Received 3 May 2001, in final form 4 October 2001
Published 21 December 2001
Online at stacks.iop.org/JPhysCM/14/319

Abstract

An explanation is proposed for a non-unique dependence of the dynamic contact angle on the wetting speed observed experimentally for some liquid–solid systems at low wetting speeds. The key idea is that the flow pattern near the wetting line, which follows from previously developed theory, suggests the possibility of a microscopic mass flux from the three-phase-interaction zone into the bulk thus causing 'imperfect rolling' of the spreading liquid. The resultant 'starvation' of the liquid–solid interface gives rise to a higher value of the contact angle. The above flow pattern turns into the regular one at a certain wetting speed thus determining the region where the metastable regimes of wetting can be observed.

1. Introduction

A few years ago Blake [1] described a specific regime of dynamic wetting, where at low contact-line speeds (about 1 mm s^{-1}) the dynamic contact angle formed by the free surface of water on polyethylene terephthalate (PET) 'began to alternate between values on a steep curve and low values on a much shallower curve. The unsteadiness died out at about 10 cm s^{-1}, and the data then rose smoothly on the shallower curve up to the maximum wetting velocity'. The data are shown as open circles in figure 1. Pictorially, the process looked as if one or more 'zippers' were moving along the contact line switching the dynamic contact angle from one value to the other [2]. The time spent by the contact angle in each position was quite macroscopic [2] and sufficient for carrying out the measurements, so that one can talk about two metastable regimes of dynamic wetting. Two important features of this phenomenon, which we should keep in mind in what follows, are that (a) it takes place for *some* gas/liquid/solid systems and (b) only at *low* contact-line speeds.

In the present paper, we try to give a possible qualitative explanation for this effect in the framework of the theory [3–6], which approaches dynamic wetting as a particular case of a more general physical phenomenon; the process by which an interface forms or disappears during flow. As a starting point, we will examine the properties of solutions of the moving contact-line problem already obtained using the simplest model formulated on the basis of the above approach. The idea is to find out whether there are regions in the parameter space specifying a gas/liquid/solid system, where at low contact-line speeds the solution exhibits

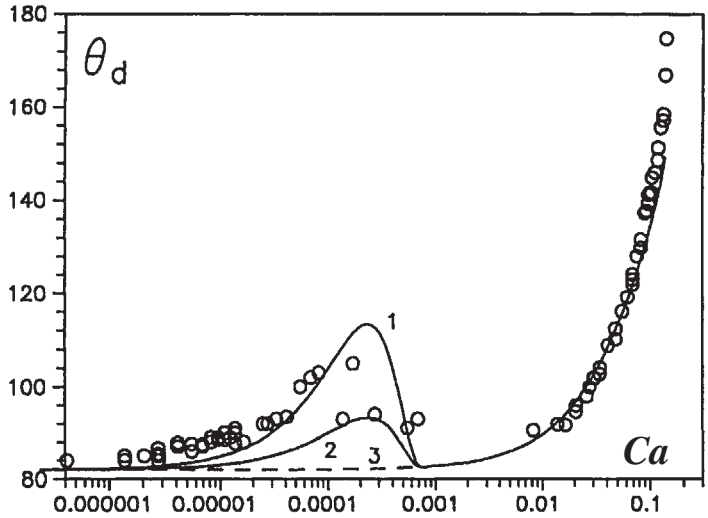

Figure 1. Experimental data for water on PET (open circles) and theoretical curves (solid curves). In the region between $Ca \approx 10^{-5}$ and $Ca \approx 10^{-3}$, the experimentally measured dynamic contact angle alternates between a steep curve and a more shallow one; the data shown in this region represent the configuration of the system for the majority of time. At the higher contact-line speeds, the contact angle rises steadily above the shallow curve. Curves 1, 2 and 3 are generated theoretically with $\alpha\beta = 0.082$ and $K_* = 5.5 \times 10^6$, 2.0×10^6 and 0, respectively.

features which could indicate the physical mechanisms responsible for metastability. Then we will consider a possible way of incorporating these mechanisms into the theory.

2. Model

First, we will briefly recapitulate the main points of the theory developed in [3–6] in its application to the simplest case of the spreading of an incompressible Newtonian liquid over a perfectly smooth chemically homogeneous solid surface. We will be considering the flow on a macroscopic (hydrodynamic) length scale where the distributions of velocity $\boldsymbol{u}$ and pressure p in the bulk are described by the Navier–Stokes equations

$$\nabla \cdot \boldsymbol{u} = 0 \qquad \rho\left(\frac{\partial \boldsymbol{u}}{\partial t} + \boldsymbol{u} \cdot \nabla \boldsymbol{u}\right) = \nabla \cdot \boldsymbol{P} \qquad \boldsymbol{P} = -p\boldsymbol{I} + \mu\left(\nabla \boldsymbol{u} + (\nabla \boldsymbol{u})^{\mathrm{T}}\right). \tag{1}$$

Here ρ and μ are the density and viscosity of the liquid; $\boldsymbol{P}$ and $\boldsymbol{I}$ are the stress and metric tensors, respectively.

The classical boundary conditions, which are normally used to specify solutions of (1) in particular flow geometries, include the no-slip condition at the solid boundary and the impermeability condition together with the balance of normal and tangential stresses acting on a liquid element at the free surface [7]. These conditions made it possible to specify a great number of solutions which accurately described numerous experimental observations. However, as is known [8], the classical formulation fails to adequately describe flows which involve moving contact lines. Indeed, in the general case, no solution to the problem exists, whilst a simplified formulation, where the normal stress boundary condition is dropped and the free-surface shape prescribed, leads to the solution exhibiting a non-integrable shear-stress singularity at the contact line [8]. In addition to this, the dynamic contact angle has to be found

as part of the solution and experiments show that its dependence on the flow and material parameters of the system is far from being trivial [1, 9].

To overcome the problem, a number of models have been proposed in the literature in the past three decades (see [6] for a comprehensive review) with the result being twofold: (a) all proposed theories remove the shear stress singularity (by introducing slip on the solid boundary of one form or another) and (b) none is able to describe the behaviour of the dynamic contact angle observed in experiments, especially the recently discovered effect of 'hydrodynamic assist' of dynamic wetting [9, 10]. It should also be mentioned that the ways in which the shear-stress singularity is removed lead to the flow kinematics in the theory being qualitatively different from what is observed in experiments, thus casting serious doubt on the very foundations of the theory.

A theory originated a decade ago [11] and developed further in [3–6] is, so far, the only one which survives the experimental tests. Its basic idea is as follows. Dynamic wetting is essentially the process by which the liquid–gas interface disappears as it passes through the three-phase-contact line and the liquid–solid interface forms[1]. This type of motion, known as 'rolling' and observed experimentally [8, 10, 12], and the resulting interface disappearance–formation process lead to the situation where the fluid particles belonging to the interface have to change their 'surface' properties (first of all the surface tension) from one equilibrium value to another. In other words, dynamic wetting is a particular case of a more general physical phenomenon, namely the process of interface formation (or/and disappearance), and has to be addressed from this viewpoint. On a macroscopic length scale, the essence of this process is the mass, momentum and energy exchange between the surface and bulk phases as a response to the variation in the equilibrium properties of the interface (which, from a microscopic point of view, result from the variation in the molecular forces experienced by the interface from the bulk phases).

Macroscopically, one can describe the mass, momentum and energy fluxes between the surface and bulk phases in the framework of irreversible thermodynamics [13, 14] and use Onsager's principle of proportionality between thermodynamic forces and fluxes to ensure positiveness of the entropy production and hence to close the set of equations. The phenomenological coefficients of proportionality introduced by this procedure have to be determined either experimentally or by considering the process on a microscopic length scale and the corresponding averaging of the microscopic quantities. The derivation sketched above is described in [3] and leads to the following boundary conditions for the Navier–Stokes equations[2]. At the free surface one has [3–5]

$$\boldsymbol{n}\cdot\boldsymbol{P}\cdot\boldsymbol{n}+p_0=\sigma_1\nabla\cdot\boldsymbol{n} \tag{2}$$

$$(\boldsymbol{I}-\boldsymbol{nn})\cdot\boldsymbol{P}\cdot\boldsymbol{n}+\nabla\sigma_1=0 \tag{3}$$

$$\sigma_1=\gamma(\rho_0^{\mathrm{s}}-\rho_1^{\mathrm{s}}) \tag{4}$$

$$\frac{\partial\rho_1^{\mathrm{s}}}{\partial t}+\nabla\cdot(\rho_1^{\mathrm{s}}\boldsymbol{v}_1^{\mathrm{s}})=-\frac{\rho_1^{\mathrm{s}}-\rho_{1\mathrm{e}}^{\mathrm{s}}}{\tau} \tag{5}$$

$$(1+4\alpha\beta)\nabla\sigma_1=4\beta(\boldsymbol{v}_1^{\mathrm{s}}-\boldsymbol{u}) \tag{6}$$

while the boundary condition at the solid surface take the form

$$(\boldsymbol{I}-\boldsymbol{nn})\cdot\boldsymbol{P}\cdot\boldsymbol{n}+\tfrac{1}{2}\nabla\sigma_2=\beta(\boldsymbol{u}-\boldsymbol{U}) \tag{7}$$

$$\sigma_2=\gamma(\rho_0^{\mathrm{s}}-\rho_2^{\mathrm{s}}) \tag{8}$$

[1] The very term 'dynamic wetting' implies formation of a 'wetted' solid surface, i.e a fresh liquid–solid interface.

[2] It should be pointed out, however, that this derivation, as well as any derivation of the mathematical model of a physical phenomenon, should be seen merely as a set of plausible self-consistent assumptions, and a reader familiar with continuum mechanics can understand the model simply by examining the boundary conditions themselves.

$$\frac{\partial \rho_2^{\rm s}}{\partial t} + \nabla \cdot (\rho_2^{\rm s} \boldsymbol{v}_2^{\rm s}) = -\frac{\rho_2^{\rm s} - \rho_{2{\rm e}}^{\rm s}}{\tau} \tag{9}$$

$$\boldsymbol{v}_2^{\rm s} = \tfrac{1}{2}(\boldsymbol{u} + \boldsymbol{U}) + \alpha \nabla \sigma_2. \tag{10}$$

Here $\boldsymbol{n}$ is the unit inward normal to the interface; p_0 is the pressure in the (inviscid) gas surrounding the fluid; σ, $\rho^{\rm s}$ and $\boldsymbol{v}^{\rm s}$ are the surface tension, surface density and the velocity with which the fluid in the surface phase is transported, respectively; $\boldsymbol{U}$ is the velocity of the solid surface; the subscripts 1 and 2 refer to the surface parameters of the liquid–gas and liquid–solid interface, respectively; $\alpha, \beta, \gamma, \tau, \rho_{1{\rm e}}^{\rm s}, \rho_{2{\rm e}}^{\rm s}$ and $\rho_0^{\rm s}$ are phenomenological constants. The surface parameters and the vector $\boldsymbol{n}$ are defined only at interfaces, so that their derivatives in the normal direction are zero.

The boundary conditions (2) and (3) at the free surface are standard; they express, respectively, the normal and tangential momentum balance of a free-surface element. Equations (4) and (8) are the equations of state in the surface phase which are taken here in the simplest form relating the surface tension and the surface density. This form is intended to reflect only the basic property of the interface, namely that its rarefaction in contact with a gas ($\rho^{\rm s} < \rho_0^{\rm s}$) corresponds to the surface *tension* whilst, in the case of a liquid–solid interface, a layer of liquid adjacent to the solid surface can be both rarefied or compressed depending on the wettability of the solid. Hence the surface tension there can be either positive or negative. The constant γ therefore is inversely proportional to the compressibility of the liquid, and $\rho_{1{\rm e}}^{\rm s}$ and $\rho_{2{\rm e}}^{\rm s}$ denote the equilibrium values of the surface density at the free-surface and liquid–solid interface, respectively. A general qualitative form of the surface equation of state is described in [3].

The surface mass balance equations (5) and (9) have a term on the right-hand side describing the mass exchange between the surface phase and the bulk. This process is driven by the difference in the chemical potentials in the surface and bulk phases and, for small deviations of the surface densities from their equilibrium values, the relaxation time τ is given by

$$\tau = \frac{1}{k_\rho \frac{{\rm d}\eta^{\rm s}}{{\rm d}\rho^{\rm s}}(\rho_{1{\rm e}}^{\rm s})}$$

where k_ρ is the Onsager coefficient associated with the mass transfer between the bulk and the surface phase and $\eta^{\rm s}$ is the chemical potential in the surface phase.

Equation (7) is the generalized Navier condition which is a direct consequence of two simple facts: (a) if inertia of an element of the liquid–solid interface is neglected, then all the forces acting on this element, that is the shear stress from the liquid, the drag force from the solid and the surface-tension gradient due to the adjacent elements of the interface, are in equilibrium, and (b) the velocity difference across the interface (as well as across any thin layer of fluid) is proportional to the external torque acting on it [15]. This physical meaning suggests that the coefficient β should be proportional to the fluid's viscosity and inversely proportional to the thickness of the layer. A comparison with experiments shows that this is indeed the case [16].

Finally, (6) and (10) relate the surface-tension gradients with the velocity in the interfacial layer and the bulk velocities evaluated at its boundaries. One can easily understand these conditions by looking at an analogy between the flow in an interface and that in a plane channel. For example, (10) has the same form as the Darcy law for flows in thin channels or porous media.

It should be emphasized that conditions (2)–(6) and (7)–(10) are the simplest ones one can self-consistently derive in the framework of the approach outlined above and the seven coefficients, γ, $\rho_0^{\rm s}$, $\rho_{1{\rm e}}^{\rm s}$, $\rho_{2{\rm e}}^{\rm s}$, α, β, τ, are the minimum one can expect. Indeed, the two

parameters γ and ρ_0^s are the minimum for the simplest (linear) equation of state in the surface phase; two constants ρ_{1e}^s and ρ_{2e}^s are required to specify the equilibrium state of the liquid–gas and liquid–solid interface, respectively; α, β and τ are associated with the Onsager coefficients corresponding to the three basic physical mechanisms, namely the response of the interface (a) to the surface-tension gradient, (b) to the external torque, and (c) the mass exchange between the interface and the bulk. No cross-effects have been taken into account. All coefficients involved have clear physical meaning and can be determined either through the corresponding microscopic modelling or from experiments. The details of the derivation, a discussion on possible generalizations of the model and the ways its parameters can be measured one can find elsewhere [3–5].

To model dynamic wetting, one has to specify conditions at the moving contact line which the functions describing distributions of the surface parameters along the interfaces must satisfy. The first condition is universal and expresses the balance of tangential projections of forces acting on the contact line as follows:

$$\sigma_1 \cos\theta_d = \sigma_{SG} - \sigma_2. \tag{11}$$

Here θ_d is the dynamic contact angle measured through the liquid. In the static situation, (11) takes the form of the classical Young's equation [17]

$$\sigma_1(\rho_{1e}^s)\cos\theta_s = \sigma_{SG} - \sigma_2(\rho_{2e}^s) \tag{12}$$

where θ_s is the static contact angle formed by the interfaces. In our case, this equation gives an extra constraint and allows one to eliminate, say, σ_{SG} and use the measurable quantity θ_s instead. It should be emphasized that (12) and, in the dynamic situation, (11) introduce the very concept of 'contact angle' into macroscopic fluid mechanics and hence have to be part of any macroscopic model of wetting phenomena.

The mass balance condition at the contact line is less trivial since it must account for various possible physical mechanisms causing mass fluxes into and out of the three-phase-interaction region, which is modelled macroscopically as the 'contact line'. It is this condition which should be subject to modifications first of all if the behaviour of the macroscopic contact angle θ_d exhibits any unusual features. In the simplest case, we can assume that the fluxes into and out of the contact line are equal as follows:

$$\rho_1^s \boldsymbol{v}_1^s \cdot \mathrm{e_f} = \rho_2^s \boldsymbol{v}_2^s \cdot \mathrm{e_g}. \tag{13}$$

Here $\mathrm{e_f}$ and $\mathrm{e_g}$ are the unit vectors normal to the contact line and tangent to the gas–liquid and gas–solid interface, respectively; $\theta_d = \arccos(-\mathrm{e_f} \cdot \mathrm{e_g})$.

One has also to formulate some conditions in the far field which will specify a particular flow.

3. 'Regular' wetting

The model outlined above makes it relatively easy to explain the main features of dynamic wetting. Since the surface-tension relaxation process is not instantaneous, the 'rolling' flow gives rise to the surface-tension gradient along the liquid–solid interface. The result is that, firstly, the values of the surface tensions at the contact line are not equal to the equilibrium values far away from it, and hence, by comparing Young's equations (11) and (12), one finds that $\theta_d \neq \theta_s$ and θ_d varies with the contact-line speed and other flow parameters. Secondly, the surface-tension gradient has a reverse influence upon the flow that caused this gradient to appear, leading to the *flow-induced* Marangoni effect. An important feature of the model is that the contact angle is linked with the distributions of the surface parameters along the interfaces

which, in their turn, are interrelated with the bulk flow. This makes the dynamic contact angle ultimately dependent on the flow near the moving contact line, that is the essence of the so-called 'hydrodynamic assist' of dynamic wetting recently discovered experimentally [9, 10]. The present model is the only one so far that accounts for this effect.

The problem formulation (1)–(13) is rather difficult to tackle mathematically and in a general case has to be treated numerically. However, there is an important case where one can arrive at useful analytical results. For steady flows, it has been shown [3–6] that, if the characteristic length scale of the flow L is large compared with the surface tension relaxation length $l = U\tau$ (U is the contact-line speed with respect to the solid surface), then in the case of small capillary numbers $Ca \equiv \mu U/\sigma_1(\rho^{\mathrm{s}}_{1\mathrm{e}}) \ll 1$, one can divide the flow domain into the following three asymptotic regions as $\epsilon \equiv l/L$ and Ca tend to zero:

(i) The 'outer' region with the characteristic length L, where (2)–(10) degenerate into the classical boundary conditions and the problem reduces to that of a flow in a corner region [18];

(ii) The 'intermediate' region with the characteristic length scale l, where the surface-tension relaxation takes place while, due to $Ca \ll 1$, viscous effects are asymptotically negligible compared to the capillary ones, and hence the interfacial properties are decoupled from those of the bulk flow;

(iii) The 'inner' or 'viscous' region with the characteristic length scale ϵl, where viscous effects become comparable with capillarity, but the asymptotically small size of this region compared to the surface-tension relaxation length, l, ensures that the variations in the surface parameters are negligible, and hence the boundary conditions at the contact line (11) and (13) can be applied to the surface distributions in the intermediate region.

As a result of the above simplifications, after standard mathematics one obtains that to the leading order the liquid–gas interface is in equilibrium up to the contact line ($\rho^{\mathrm{s}} \equiv \rho^{\mathrm{s}}_{1\mathrm{e}}$) and the velocity with which the free surface enters the three-phase-interaction region (i.e. the 'contact line') is equal to that in the outer region. The latter is well known [18] and, scaled with the contact-line speed U, is given by

$$\bar{u}_0(\theta_{\mathrm{d}}) = \frac{\sin\theta_{\mathrm{d}} - \theta_{\mathrm{d}}\cos\theta_{\mathrm{d}}}{\sin\theta_{\mathrm{d}}\cos\theta_{\mathrm{d}} - \theta_{\mathrm{d}}}. \tag{14}$$

Then the problem of modelling the contact-angle behaviour becomes reduced to finding the distributions of the surface parameters along the liquid–solid interface in the intermediate region from a set of ordinary differential equations resulted from (7)–(10), where the term $(\boldsymbol{I} - \boldsymbol{nn}) \cdot \boldsymbol{P} \cdot \boldsymbol{n}$, being proportional to Ca, is neglected, $\boldsymbol{u}$ is eliminated and σ_2 expressed in terms of ρ^{s}_2 using (8) as follows:

$$\frac{\mathrm{d}(\bar{\rho}^{\mathrm{s}}_2\bar{v}^{\mathrm{s}}_2)}{\mathrm{d}r} = -(\bar{\rho}^{\mathrm{s}}_2 - \bar{\rho}^{\mathrm{s}}_{2\mathrm{e}}) \tag{15}$$

$$\frac{\mathrm{d}\bar{\rho}^{\mathrm{s}}_2}{\mathrm{d}r} = 4V^2(1 - \bar{v}^{\mathrm{s}}_2). \tag{16}$$

Here r is the distance from the contact line scaled with the surface-tension relaxation length l, $\bar{\rho}^{\mathrm{s}}_2 = \rho^{\mathrm{s}}_2/\rho^{\mathrm{s}}_0$, $\bar{v}^{\mathrm{s}}_2 = v^{\mathrm{s}}_2/U$ and

$$V = U\left(\frac{\tau\beta}{\gamma\rho^{\mathrm{s}}_0(1 + 4\alpha\beta)}\right)^{1/2} \tag{17}$$

is the dimensionless contact-line speed. The solution of (15) and (16) must satisfy the equilibrium condition in the far field

$$\bar{\rho}^{\mathrm{s}}_2 \to \bar{\rho}^{\mathrm{s}}_{2\mathrm{e}} \qquad \text{as} \quad r \to +\infty \tag{18}$$

together with the boundary conditions (11) and (13) which now take the form

$$\cos\theta_{\rm d} - \cos\theta_{\rm s} = \frac{\bar\rho_2^{\rm s}(0) - \bar\rho_{2{\rm e}}^{\rm s}}{1 - \bar\rho_{1{\rm e}}^{\rm s}} \tag{19}$$

$$\bar\rho_2^{\rm s}(0)\bar v_2^{\rm s}(0) = -\bar\rho_{1{\rm e}}^{\rm s}\bar u_0(\theta_{\rm d}) \tag{20}$$

where $\bar\rho_{1{\rm e}}^{\rm s} = \rho_{1{\rm e}}^{\rm s}/\rho_0^{\rm s}$ and $\bar u_0(\theta_{\rm d})$ is given by (14). The three conditions (18)–(20) allow one to determine two constants of integration together with $\theta_{\rm d}$. For small deviations of $\bar\rho_2^{\rm s}$ from $\bar\rho_{2{\rm e}}^{\rm s}$ one can simplify the problem even further, linearize (15)–(20) and arrive at an analytical relationship between V and $\theta_{\rm d}$ of the following form:

$$V = \tfrac{1}{2}G\left(\frac{\bar\rho_{2{\rm e}}^{\rm s}}{F(F-G)}\right)^{1/2} \tag{21}$$

where

$$F = \frac{\bar\rho_{2{\rm e}}^{\rm s} + \bar\rho_{1{\rm e}}^{\rm s}\bar u_0(\theta_{\rm d})}{1 - \bar\rho_{1{\rm e}}^{\rm s}} \qquad G = \cos\theta_{\rm s} - \cos\theta_{\rm d}.$$

If the gas-to-liquid viscosity ratio k_μ has to be taken into account ($\theta_{\rm d}$ is sufficiently close to 180°) (21) will still be valid with contributions from the outer solution $\bar u_0(\theta_{\rm d})$ replaced by its generalization [6]

$$\bar u_0(\theta_{\rm d}, k_\mu) = \frac{(\sin\theta_{\rm d} - \theta_{\rm d}\cos\theta_{\rm d})K(\theta_2) - k_\mu(\sin\theta_2 - \theta_2\cos\theta_2)K(\theta_{\rm d})}{(\sin\theta_{\rm d}\cos\theta_{\rm d} - \theta_{\rm d})K(\theta_2) + k_\mu(\sin\theta_2\cos\theta_2 - \theta_2)K(\theta_{\rm d})} \tag{22}$$

where $\theta_2 = \pi - \theta_{\rm d}$ and $K(\theta) = \theta^2 - \sin^2\theta$. Then, $\bar u_0(\theta_{\rm d})$ given by (14) becomes just $\bar u_0(\theta_{\rm d}, 0)$ in (22).

The velocity dependence of the dynamic contact angle given by (21) is shown to be in good agreement with experiments for different liquids in the absence of metastability [3, 6].

4. Metastability

Clearly, (21) sets a one-to-one correspondence between the contact-line speed (V or Ca) and the dynamic contact angle $\theta_{\rm d}$ for the given values of parameters and a given overall flow geometry (the latter manifests itself in $\bar u_0$ that comes from the solution for a flow in a wedge region). However, experiments reported in [1] show that for some fluids there exists a interval of the contact-line speeds where dynamic wetting exhibits rather unusual features. The process becomes unsteady and the contact angle starts to alternate between two different values (figure 1). The frequency of these oscillations is small compared with $1/\tau$ so that, from the point of view of the interface formation, these two contact angles can be regarded as corresponding to two steady metastable regimes of wetting. One can plot the data in the same $\theta_{\rm d}$ versus Ca coordinate plane (figure 1) having in mind that, as the contact-line speed increases, the contact angle spends less and less time on the steep curve until the metastability finally dies out and the process becomes steady again with the contact angle rising along the shallow curve.

In an attempt to understand and macroscopically describe the metastable regimes, we can employ the theory of dynamic wetting as an interface formation process, that provides not only the simplest mathematical model outlined above but, more importantly, the conceptual framework for generalizations incorporating extra physical mechanisms. One can look for a clue to what is observed in experiments in the flow patterns associated with the regions in the parameter space which could be correlated with the conditions under which the metastability takes place.

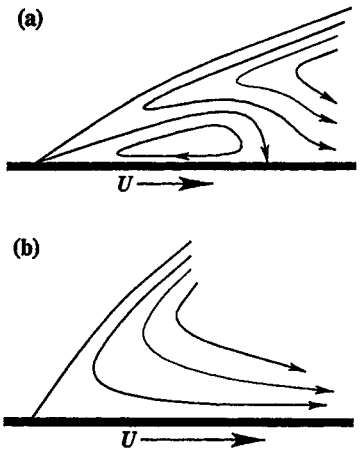

Figure 2. Flow patterns: (a) with a vortex near the contact line occurring in a certain range of the parameter space at low contact-line speeds only; (b) a regular-flow pattern. The flow associated with the separating stream line can cause a 'leak' from the origin.

An interesting peculiarity of the flow field reported earlier [5] is that, besides a regular pattern shown in figure 2(b), in a certain region of the parameter space (that is physically for *some* gas/liquid/solid systems) and only at *low* contact-line speeds, the theory predicts a flow pattern shown in figure 2(a). In this case, there appears a vortex near the contact line, and one of the stream lines comes out from the origin[3]. The physical reason behind this macroscopic feature is the flow-induced Marangoni effect. The overall rolling motion of the fluid gives rise to a surface-tension gradient along the liquid–solid interface which in its turn influences the flow. The main effect of the surface-tension gradient is on the velocity distribution on the liquid-facing side of the liquid–solid interface, which is the boundary condition for the bulk flow. For the given distributions of the surface parameters, this boundary condition follows from (10).

For some liquids at low contact angles the effect of the surface tension gradient is so strong compared to the bulk flow that it causes a reverse flow on the liquid-facing side of the liquid–solid interface, thus creating a vortex near the moving contact line. Schematically, the flow in the interfacial layers is shown in figure 3: convergent flow towards the contact line on the liquid-facing sides of interfaces gives rise to a flow directed away from the contact line.

As the contact-line speed increases, the recirculation region contracts and eventually disappears giving way to the regular flow pattern shown in figure 2(b).

A qualitative resemblance between the conditions required for the vortex near the moving contact line to appear in the theory and those associated with the metastable regimes of wetting described in the experiments [1] suggests looking at the former for a physical mechanism responsible for the latter. More specifically, it seems reasonable to assume that the flow pattern shown in figure 2(a) can trigger an additional mass flux out of the viscous region which should be taken into account while applying condition (11) to the inner limits of the distributions of the surface parameters in the intermediate region. To put it pictorially, the flow from the origin will tend to 'suck' fluid from the interface into the bulk thus affecting the surface mass balance condition (13) and through (4), (11) influencing the dynamic contact angle. This argument

[3] For a flow in the intermediate region (2 in figure 3), the 'origin' is the viscous region (3 in figure 3) and not the contact line itself.

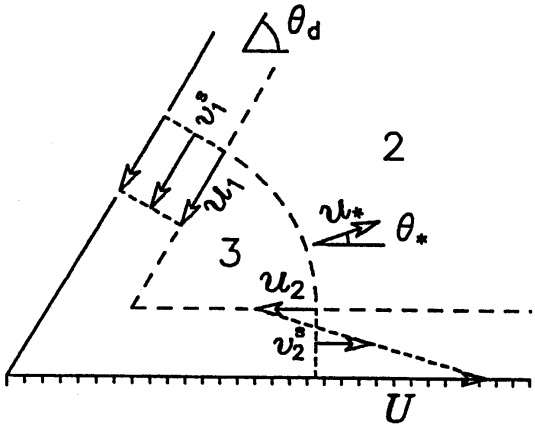

Figure 3. A definition sketch for the flow-induced Marangoni effect. The fluid particles initially belonging to the free surface are driven through the three-phase-interaction region and become elements of the liquid–solid interface. The resulting surface-tension gradient along the this interface affects the velocity distribution in the interfacial layer. For some regimes this effect causes the reverse flow on the liquid-facing side of the interface thus giving rise to the recirculation zone shown in figure 2(a).

suggests replacing (13) with the condition

$$\rho_1^s \boldsymbol{v}_1^s \cdot \mathrm{e_f} = \rho_2^s \boldsymbol{v}_2^s \cdot \mathrm{e_g} + W \tag{23}$$

where W is an additional mass flux, that is a 'leak' from the interface into the bulk. This mass flux should depend on the same factors as those causing the recirculation. We can use the dimensionless velocity at the origin on the separating stream line u_* (see figures 2(a), 3) as a measure of recirculation. Then, by correlating W with u_* one will model the effect of 'sucking' the fluid from the origin into the bulk.

In the formulation (1)–(11) u_* is a function of five parameters $u_* = f(V, \theta_s, \rho_{1e}^s, \sigma_{SG}, \alpha\beta)$. It can be calculated as follows. Once $\bar{v}_2^s$ and $\bar{\rho}_2^s$ (and hence σ_2) are known from (15)–(20), one can find from (10) the bulk velocity on the liquid-facing side of the liquid–solid interface $\bar{u}$ as a function of r. For this function one has

$$\lim_{r\to 0} \bar{u}(r) = 1 - \frac{(1-\bar{\rho}_{1e}^s)(\cos\theta_s - \cos\theta_d)[(V^2+\bar{\rho}_{2e}^s)^{1/2} - V]}{V\bar{\rho}_{2e}^s(1+4\alpha\beta)}. \tag{24}$$

Thus, to find the flow near the origin one has to solve the biharmonic equation

$$\left[\frac{1}{r}\frac{\partial}{\partial r}\left(r\frac{\partial}{\partial r}\right) + \frac{1}{r^2}\frac{\partial^2}{\partial\theta^2}\right]^2 \psi = 0$$

for the stream function ψ, introduced by

$$u_r = \frac{1}{r}\frac{\partial\psi}{\partial\theta} \qquad u_\theta = -\frac{\partial\psi}{\partial r}$$

(u_r, u_θ are, respectively, the radial and transversal components of the bulk velocity), in a wedge region $0 < \theta < \theta_d$, $0 < r < +\infty$ subject to the following boundary conditions:

$$\begin{aligned} &\psi(r,0) = \psi(r,\theta_d) = 0 \\ &\frac{1}{r}\frac{\partial\psi}{\partial\theta}(r,\theta_d) = u_1 = \bar{u}_0(\theta_d) \\ &\frac{1}{r}\frac{\partial\psi}{\partial\theta}(r,0) = u_2 = 1 - \frac{(1-\rho_{1e}^s)(\cos\theta_s - \cos\theta_d)[(V^2+\rho_{2e}^s)^{1/2} - V]}{V\rho_{2e}^s(1+4\alpha\beta)}. \end{aligned} \tag{25}$$

The solution to this problem can easily be found in the form $\psi = r\,F(\theta)$, where $F(\theta) = -2C_1 \sin^2\theta + C_2 \sin 2\theta + C_3\theta$, and the constants C_1, C_2, C_3 are given by

$$C_1 = \frac{u_1(\sin 2\theta_d - 2\theta_d) + u_2(2\theta_d \cos 2\theta_d - \sin 2\theta_d)}{8\sin\theta_d(\theta_d\cos\theta_d - \sin\theta_d)}$$

$$C_2 = \frac{u_1 \sin\theta_d + u_2(2\theta_d - \sin\theta_d)}{4(\theta_d\cos\theta_d - \sin\theta_d)} \qquad C_3 = \frac{2\sin^2\theta_d}{\theta_d}C_1 - \frac{\sin 2\theta_d}{\theta_d}C_2.$$

Then, the angle θ_* formed by the separating stream line at the origin and the solid surface is determined from $F(\theta_*) = 0$ and the velocity we are looking for is given by

$$u_*(\theta_*) = F'(\theta_*). \tag{26}$$

Now one can replace (13) for the inner limits of the distributions in the intermediate region with (23) and use

$$W = K_* u_*^2(\theta_*) \tag{27}$$

as a simple dependence of the flux into the bulk, W, on the measure of the rate of recirculation u_*. Replacing (20) with (23), (27), where u_* is given by (26), one arrives at a qualitative behaviour of the θ_d versus V theoretical curve similar that observed experimentally.

Although the goal of the present work is to look for the physical mechanisms responsible for metastability at a qualitative level, it is interesting to attempt to fit the macroscopic dependence of θ_d on Ca to the experimental data 'semi-quantitatively', ie by using K_* and $\alpha\beta$ as adjustable parameters. This attempt can be carried out in the following two steps. Firstly, one can fit the theoretical curve generated by (15)–(20), ie with $K_* = 0$, to the data in figure1 corresponding to stable high-velocity wetting ($Ca > 0.01$). This can be done by employing the procedure described in [3] and specifying the values of $\bar{\rho}^s_{1e}$ (= 0.59), $\bar{\sigma}_{SG}$ (= 0) and the scaling factor $Sc = V/Ca$ (= 4.17), that relates the contact-line speed scaled with the surface parameters of the model (17) to the capillary number, which is effectively the contact-line speed scaled with $\sigma_{1e}\mu^{-1}$. To account for the gas-to-fluid viscosity ratio (=0.0181), we used (22) instead of (14).

The second step is to keep the values of $\bar{\rho}^s_{1e}$, $\bar{\sigma}_{SG}$ and Sc determined in the first step, replace (20) with (23), (27) and use $\alpha\beta$ and K_* as adjustable constants trying to describe the whole set of experimental data presented in figure 1, including the region corresponding to metastable regimes. The parameter K_* will then affect only the maximum value θ_{meta} reached by the contact angle in the metastable region. The product $\alpha\beta$, which influences u_* via (25), also affects θ_{meta} through (27) and it is the only factor determining the velocity at which u_* becomes equal to zero and hence the metastability dies out.

The results of the above two-step procedure are shown in figure 1. Curves 1, 2 and 3 correspond to $\alpha\beta = 0.082$ and $K_* = 5.5 \times 10^6$, 2×10^6 and 0, respectively. One can see that the curves in figure 1 do describe the behaviour of the experimental data. Interestingly, the value of $\alpha\beta = 0.082$ is only 2% smaller than $1/12$, which would follow from the analogy between the flow in the interfacial layer and the Couette–Poiseuille flow in a plane channel [3].

It should be emphasized that the qualitative agreement between theory and experiment is not specific to the form (23) chosen for W; qualitatively similar results can be obtained using any smooth monotonically increasing function $W(u_*)$ instead. The reason is that, in dimensional terms, the recirculation zone increases with Uu_* and hence between the limits $U = 0$ (no motion) and $u_* = 0$ (no recirculation, figure 2(a)) any monotonically increasing function $W(u_*)$ will give rise to a branch in the θ_d-versus-Ca plane with a higher value of θ_d than for $W \equiv 0$.

5. Discussion

It is clear that, since metastability of dynamic wetting manifests itself through the behaviour of the macroscopic dynamic contact angle, which in turn is determined by the balance of the surface forces acting on the three-phase-contact line, one has to look into processes in this region for the ultimate cause of the metastability. The present work suggests that the macroscopic outcome of the processes in the three-phase-interaction zone is that the transition of the liquid–gas interface into the liquid–solid one can take place with sporadic losses of the 'interfacial material' into the bulk and the resulting 'starvation' of the forming liquid–solid interface. This creates extra tension which drives the contact angle up. According to the present results, the release of the fluid particles belonging to the interface into the bulk can be triggered by the Marangoni effect on the liquid–solid interface and hence should be broadly proportional to the factors responsible for this effect. What macroscopic theory cannot answer is what the nature of this proportionality is, what microscopic mechanisms compete in the region of the parameter space where the metastability is observed, and what physical properties of the gas-liquid–solid system determine the effect quantitatively. Blake's tentative explanation of the effect [1] in terms of his molecular-kinetic theory [19] refers to a possibility of 'strong' or 'weak' interactions respectively of a fewer or greater number of the fluid's molecules with the solid being the reason for the two regimes observed experimentally. This explanation, that is broadly compatible with the macroscopic picture given in the present work, can perhaps be seen as an insight into and a step towards the understanding of the microscopic nature of this type of metastability but, of course, not as the solution to the problem. The questions raised in this paper require a comprehensive study on the microscopic level, perhaps, by means of statistical physics or molecular-dynamics simulations.

Finally, it should be pointed out that, according to previous experiments [9], the dynamic contact angle is dependent on the flow field in the bulk. Theoretically, this follows from the fact that the macroscopic contact angle is determined by the balance of the surface tensions acting on the contact line (11) whilst the surface-tension distributions along the interfaces are linked to the shear stress by the conditions requiring the balance of forces acting on every element of the interface (3), (7). The way in which the metastable regimes of wetting are addressed in the present paper indicates that one should perhaps look at the role played by the *normal* stress and its influence on the mass exchange between the interface and the bulk. The model's derivation [3] suggests that the normal stresses can act together with the difference of the chemical potentials in the surface and bulk phase which makes this idea plausible. The problem then is how to apply this general idea to the possibility of a mass flux from the three-phase-interaction zone, where, strictly speaking, one can specify only the limits of the surface parameter distributions. This issue is also beyond the reach of continuum mechanics modelling and has to be addressed from a microscopic point of view.

References

[1] Blake T D 1993 Dynamic contact anles and wetting kinetics *Wettability* ed J C Berg (New York: Dekker)
[2] Blake T D 1995 Personal communication
[3] Shikhmurzaev Y D 1993 The moving contact line on a smooth solid surface *Int. J. Multiphase Flow* **19** 589
[4] Shikhmurzaev Y D 1994 Mathematical modelling of wetting hydrodynamics *Fluid Dynam. Res.* **13** 45
[5] Shikhmurzaev Y D 1996 Dynamic contact angles and flow in vicinity of moving contact line *AIChE J.* **42** 601
[6] Shikhmurzaev Y D 1997 Moving contact lines in liquid/liquid/solid systems *J. Fluid Mech.* **334** 211
[7] Batchelor G K 1967 *An Introduction to Fluid Dynamics* (Cambridge: Cambridge University Press)
[8] Dussan V E B 1979 On the spreading of liquids on solid surfaces: static and dynamic contact lines *A. Rev. Fluid Mech.* **11** 371

[9] Blake T D, Bracke M and Shikhmurzaev Y D 1999 Experimental evidence of nonlocal hydrodynamic influence on the dynamic contact angle *Phys. Fluids* **11** 1995
[10] Blake T D, Clarke A and Ruschak K J 1994 Hydrodynamic assist of dynamic wetting *AIChE J.* **40** 229
[11] Shikhmurzaev Y D 1991 Spreading flow of a viscous liquid over a solid surface *Sov. Phys.–Dokl.* **36** 749
[12] Dussan V E B and Davis S H 1974 On the motion of a fluid–fluid interface along a solid surface *J. Fluid Mech.* **65** 71
[13] de Groot S R and Mazur P 1962 *Non-Equilibrium Thermodynamics* (Amsterdam: North-Holland)
[14] Bedeaux D, Albano A M and Mazur P 1976 Boundary conditions and non-equilibrium thermodynamics *Physica* A **82** 438
[15] Barenblatt G I and Chernyi G G 1963 On moment relations on surfaces of discontinuity in dissipative media *PMM* **27** 784
[16] Shikhmurzaev Y D 1997 Spreading of drops on solid surfaces in a quasi-static regime *Phys. Fluids* **9** 266
[17] Young T 1805 An essay on the cohesion of fluids *Phil. Trans. R. Soc.* **95** 65
[18] Moffatt H K 1964 Viscous and resistive eddies near a sharp corner *J. Fluid Mech.* **18** 1
[19] Blake T D and Haynes J M 1969 Kinetics of liquid/liquid displacement *J. Colloid Interf. Sci.* **30** 421